PAR1 agonists stimulate APC-like endothelial cytoprotection and confer resistance to thromboinflammatory injury

Karen De Ceunynck[a,1], Christian G. Peters[a,1], Abhishek Jain[b,2], Sarah J. Higgins[c,d], Omozuanvbo Aisiku[a], Jennifer L. Fitch-Tewfik[a], Sharjeel A. Chaudhry[a], Chris Dockendorff[e], Samir M. Parikh[c,d], Donald E. Ingber[b,f,g,h], and Robert Flaumenhaft[a,3]

[a]Division of Hemostasis and Thrombosis, Department of Medicine, Beth Israel Deaconess Medical Center, Harvard Medical School, Boston, MA 02115; [b]Wyss Institute for Biologically Inspired Engineering, Harvard University, Boston, MA 02115; [c]Division of Nephrology, Department of Medicine, Beth Israel Deaconess Medical Center, Harvard Medical School, Boston, MA 02115; [d]Center for Vascular Biology Research, Department of Medicine, Beth Israel Deaconess Medical Center, Harvard Medical School, Boston, MA 02115; [e]Department of Chemistry, Marquette University, Milwaukee, WI 53201; [f]Vascular Biology Program, Boston Children's Hospital and Harvard Medical School, Boston, MA 02115; [g]Department of Surgery, Boston Children's Hospital and Harvard Medical School, Boston, MA 02115; and [h]Harvard John A. Paulson School of Engineering and Applied Sciences, Harvard University, Cambridge, MA 02138

Edited by Barry S. Coller, The Rockefeller University, New York, NY, and approved December 18, 2017 (received for review November 1, 2017)

Stimulation of protease-activated receptor 1 (PAR1) on endothelium by activated protein C (APC) is protective in several animal models of disease, and APC has been used clinically in severe sepsis and wound healing. Clinical use of APC, however, is limited by its immunogenicity and its anticoagulant activity. We show that a class of small molecules termed "parmodulins" that act at the cytosolic face of PAR1 stimulates APC-like cytoprotective signaling in endothelium. Parmodulins block thrombin generation in response to inflammatory mediators and inhibit platelet accumulation on endothelium cultured under flow. Evaluation of the antithrombotic mechanism showed that parmodulins induce cytoprotective signaling through Gβγ, activating a PI3K/Akt pathway and eliciting a genetic program that includes suppression of NF-κB–mediated transcriptional activation and up-regulation of select cytoprotective transcripts. *STC1* is among the up-regulated transcripts, and knockdown of stanniocalin-1 blocks the protective effects of both parmodulins and APC. Induction of this signaling pathway in vivo protects against thromboinflammatory injury in blood vessels. Small-molecule activation of endothelial cytoprotection through PAR1 represents an approach for treatment of thromboinflammatory disease and provides proof-of-principle for the strategy of targeting the cytoplasmic surface of GPCRs to achieve pathway selective signaling.

endothelium | cytoprotection | thrombosis | inflammation | PAR1

Protease-activated receptor 1 (PAR1) is a multifunctional G-protein–coupled receptor (GPCR) that is activated by proteolytic cleavage and couples to several G proteins. It was originally identified as the receptor for thrombin (1) and was subsequently found to be a substrate for multiple vascular proteases, including other serine proteases as well as metalloproteases (2–6). The activation mechanism of PARs is unique among GPCRs. Cleavage at a GPCR's N terminus reveals a tethered ligand that interacts with a shallow binding site on the extracellular surface of the receptor (1, 7). This intramolecular activation mechanism results in a conformational change that is transmitted to cognate G proteins, including Gαq, Gαi, Gα13, and Gγβ as well as to β-arrestin (8–12). PAR1 is the most abundant GPCR on platelets and serves a critical role in linking activation of the coagulation cascade with platelet activation. PAR1 is also found on endothelium, where it can stimulate either inflammatory signaling or antiinflammatory signaling depending on the activating protease and physiological context (13). Typically, thrombin induces proinflammatory signaling. However, cleavage of PAR1 by alternative proteases, such as activated protein C (APC), can protect endothelial cells from inflammatory mediators (14–17).

APC-mediated cytoprotection may also render endothelium resistant to prothrombotic stimuli. Proteolysis of PAR1 by APC results in the generation of a unique tethered ligand that stimulates antiinflammatory, antiapoptotic, and barrier function fortifying pathways in endothelium (10, 18–23). Antithrombotic activity may also be a component of this response. However, evaluation of the ability of APC-mediated PAR1 stimulation to oppose prothrombotic effects of inflammatory stimuli has been complicated by its opposing activities on coagulation factors that associate with endothelium. On one hand, APC cleaves the kunitz domain of tissue factor pathway inhibitor, augmenting tissue factor activity on endothelium (24). On the other hand APC cleaves factor V and VIII (25, 26), thus inhibiting thrombin generation. Understanding whether cytoprotective signaling confers endothelium with an antithrombotic phenotype is important since this pathway could be a useful target for preventing thrombosis that frequently accompanies inflammatory conditions.

Using a high-throughput screening approach, we previously identified an antithrombotic class of small-molecule PAR1

Significance

Protease-activated receptors (PARs) are G-protein–coupled receptors (GPCRs) that are activated by proteolysis and couple to multiple distinct G-proteins. Cleavage of PAR1 in endothelium stimulates either proinflammatory or antiinflammatory signaling depending on the activating protease and is important in thrombosis and inflammation. Yet the biased signaling of PAR1 has made its pharmacological modulation challenging. We show that a family of compounds, parmodulins, acts at the cytosolic face of PAR1 to differentially control G-protein coupling and stimulate cytoprotective signaling while blocking deleterious signaling. Parmodulins are antiinflammatory and antithrombotic in vivo. These compounds demonstrate the utility of targeting the cytosolic face of GPCRs to selectively modulate downstream signaling and could provide an alternative for treatment of thromboinflammatory disorders.

Author contributions: K.D.C., C.G.P., A.J., S.J.H., O.A., J.L.F.-T., D.E.I., and R.F. designed research; K.D.C., C.G.P., A.J., S.J.H., O.A., J.L.F.-T., and S.A.C. performed research; C.D. contributed new reagents/analytic tools; K.D.C., C.G.P., A.J., S.A.C., C.D., S.M.P., D.E.I., and R.F. analyzed data; and K.D.C., C.G.P., A.J., S.M.P., D.E.I., and R.F. wrote the paper.

Conflict of interest statement: R.F. and C.D. are inventors on a patent describing parmodulins.

This article is a PNAS Direct Submission.

[1]K.D.C. and C.G.P. contributed equally to this work.

[2]Present address: Department of Biomedical Engineering, Dwight Look College of Engineering, Texas A&M University, College Station, TX 77843.

[3]To whom correspondence should be addressed. Email: rflaumen@bidmc.harvard.edu.

This article contains supporting information online at www.pnas.org/lookup/suppl/doi:10.1073/pnas.1718600115/-/DCSupplemental.

modulators, termed "parmodulins," which act at the cytoplasmic face of PAR1 (27–29). Characterization of these compounds showed that they are antithrombotic in vivo (27, 29). We hypothesized that modulation of endothelial function is an important determinant of the antithrombotic effect of parmodulins. The protective effects of parmodulins were evaluated on endothelial cells in vitro and in mouse models of thromboinflammation. We found that parmodulins blocked thrombin generation on endothelial cells induced by inflammatory mediators such as TNF-α and lipopolysaccharide (LPS) despite their selectivity for PAR1. In mouse models of thromboinflammation, parmodulins demonstrate an antithrombotic effect at the level of endothelium that is independent of its antiplatelet activity. Evaluation of this phenomenon showed that parmodulins blocked proinflammatory responses and co-opted an APC-like cytoprotective pathway downstream from PAR1. Thus, parmodulins stimulate cytoprotective signaling through PAR1 even as they block PAR1-mediated proinflammatory signaling. These compounds provide proof-of-principle for the strategy of targeting the cytoplasmic face of GPCRs to achieve pathway selective signaling.

Results

Parmodulins Stimulate Antithrombotic Signaling Through Endothelial PAR1. Prior work identifying PAR1 modulators led to the identification of parmodulins, which block platelet activation through PAR1, but not activation mediated through PAR4 or several other platelet GPCRs (27–29). Experiments using mutant and chimeric PARs as well as radiolabeled PAR1 ligands demonstrated that these compounds act at the cytosolic face of PAR1 (27, 29). In functional studies, parmodulins demonstrated biased activity with regard to G-protein coupling, inhibiting PAR1-mediated signaling through $G\alpha_q$, but not $G\alpha_{12/13}$, in platelets and endothelium (Fig. S1) (28, 29). While we have previously shown that parmodulins inhibit PAR1-mediated prothrombotic responses in platelets (28, 29), their effect on endothelial-cell prothrombotic responses was unknown. We therefore tested whether parmodulins could block thrombin generation induced by LPS or tumor necrosis factor-α (TNF-α), two inflammatory mediators known to induce thrombotic responses in endothelium (30–32). Incubation of human umbilical vein endothelial cells (HUVECs) with parmodulin 2 (2-Bromo-*N*-[3-[(1-oxobutyl)amino]phenyl] benzamide; ML161) (28) for 4 h inhibited LPS-induced thrombin generation by 70 ± 15% and TNF-α–induced thrombin generation by 53 ± 9.9% (Fig. 1*A* and Fig. S2*A*). Consistent with its known anticoagulant activity, APC also inhibited LPS-induced thrombin generation (Fig. S2*B*). APC interferes with thrombin generation by cleaving factors V and VIII (25, 26). To determine whether the antithrombotic effect of parmodulin 2 was secondary to inhibition of coagulation proteins via an off-target activity, we tested whether parmodulin 2 prolonged the activated partial thromboplastin time (aPTT), a

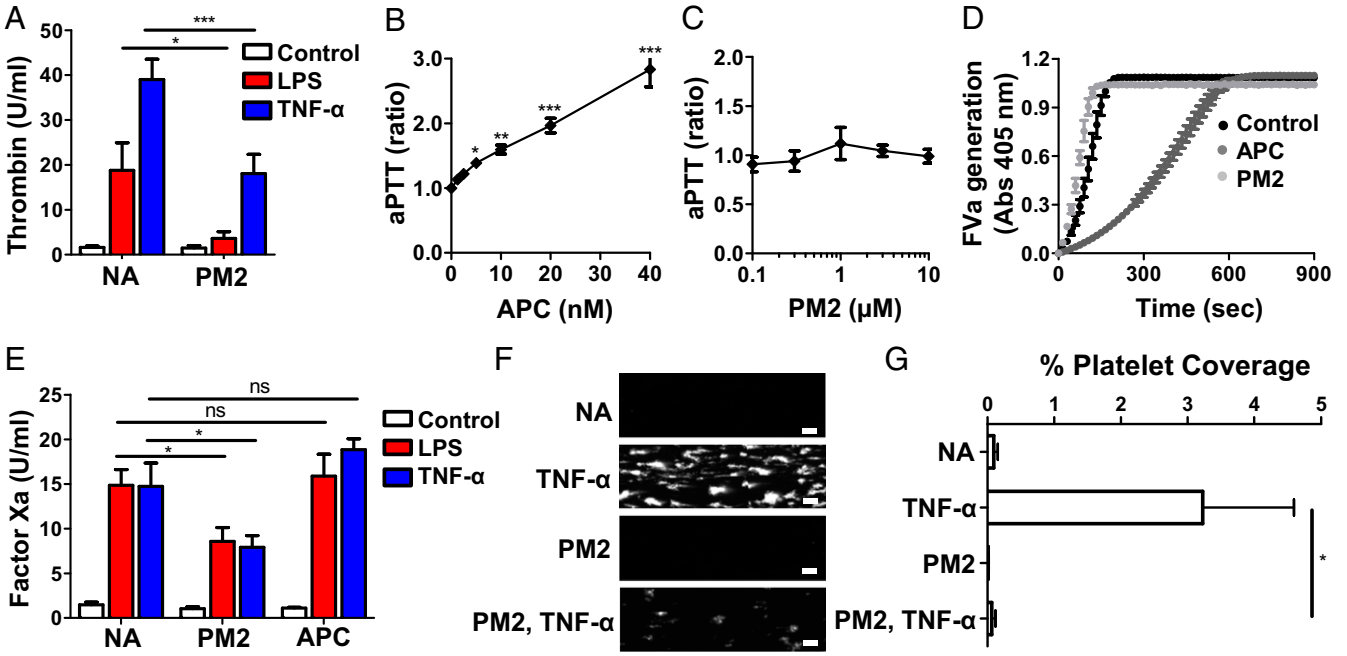

Fig. 1. A biased PAR1 agonist is thromboprotective at the level of endothelium. (*A*) Effect of PM2 on LPS- and TNF-α–induced thrombin generation. HUVECs were preincubated with vehicle (NA) or PM2 (3 μM) for 4 h. Samples were either left untreated (control) or then exposed to TNF-α (10 ng/mL) or LPS (100 ng/mL) for an additional 4 and 3 h, respectively. Thrombin generation was monitored using a fluorogenic thrombin substrate. Values are normalized to controls and depicted as mean ± SEM ($n \geq 6$). One-way ANOVA with Bonferroni posttests was used to compare groups. *$P < 0.05$; ***$P < 0.001$. (*B* and *C*) Comparison of the dose dependency of (*B*) APC and (*C*) PM2 in an aPTT assay. Clotting times are represented as the ratio of samples containing APC or PM2 versus control samples. Data represent mean ± SEM of seven samples normalized to control samples. A matched one-way ANOVA with Bonferroni posttests was used to compare PM2- and APC-treated groups to control. *$P < 0.05$; **$P < 0.01$, ***$P < 0.001$. (*D*) Effect of PM2 and APC on FVa generation. HUVECs were incubated with PM2 (10 μM) for 4 h and APC (10 nM) for 15 min. FVa generation was measured using a chromogenic substrate and depicted as a function of time. Representative experiment of three independent experiments. (*E*) HUVECs were preincubated with vehicle (NA), PM2 (3 μM), or APC (10 nM) for 4 h. Samples were either left untreated (control) or then exposed to TNF-α (10 ng/mL) or LPS (100 ng/mL) for an additional 4 and 3 h, respectively. Factor Xa generation was monitored using a chromogenic FXa substrate. Values are normalized to controls and depicted as mean ± SEM ($n \geq 6$). One-way ANOVA with Bonferroni posttests was used to compare groups. *$P < 0.05$. (*F* and *G*) Bioengineered microvessels were perfused with either vehicle [No addition (NA), TNF-α] or parmodulin 2 (PM2; PM2, TNF-α) for 4 h. Samples were subsequently washed and perfused with whole blood containing either buffer alone (NA, PM2) or TNF-α (TNF-α; PM2, TNF-α). Platelet accumulation on endothelial monolayers was detected using an anti-CD41-PE antibody and visualized by videomicroscopy. (Scale bar: 100 μm.) (*F*) A composite image made from separate micrographs of an endothelial cell surface is shown. Separate fields have been spliced together to create the image. (*G*) Quantification of TNF-α–induced platelet accumulation on endothelium. Data represent mean ± SEM ($n = 3$–5). The *t*-tests were used for statistical analysis to compare TNF-α and PM2, TNF-α groups. *$P < 0.05$. ns, nonsignificant.

plasma-based coagulation assay. However, unlike APC, which is an anticoagulant and prolongs the aPTT (Fig. 1*B*), parmodulin 2 had no effect on the aPTT (Fig. 1*C*). Neither parmodulin 2 nor APC had any effect on prothrombin time (PT) (Fig. S2 *C* and *D*).

To further distinguish the antithrombotic activity of APC from that of parmodulin 2 at the level of the endothelium, we compared their effects in factor V and factor X activation assays. In the factor V assay, incubation with APC resulted in significant inhibition, whereas incubation with parmodulin 2 had no significant effect (Fig. 1*D*). In a plasma-free factor X activation assay, both LPS and TNF-α induce tissue factor expression in endothelium, thereby enhancing the generation of factor Xa (Fig. 1*E* and Fig. S2*E*) (33–35). Incubation with parmodulin 2 for 4 h before LPS or TNF-α exposure inhibited factor Xa generation by 45 ± 10% and 52 ± 6%, respectively (Fig. 1*E* and Fig. S2*E*). In contrast, incubation with APC alone had little effect on either LPS or TNF-α–induced factor Xa generation on endothelium (Fig. 1*E* and Fig. S2*F*), possibly owing to the ability of APC to cleave tissue factor pathway inhibitor (24), thereby preventing inhibition of tissue factor. We have previously shown that incubation of endothelium with parmodulin 2 for 30 min is sufficient to inhibit $G\alpha_q$ signaling in endothelium (29). This relatively short exposure, however, did not inhibit LPS-induced factor Xa generation (Fig. S2 *G* and *H*). This result suggested that parmodulin 2-mediated inhibition of endothelial PAR1 was not responsible for blocking thrombin generation on endothelium. Of note, the ability of APC to elicit cytoprotective signaling in endothelial cells requires transcriptional activation and therefore necessitates prolonged exposures (>3 h) (14, 36). These observations raised the possibility that parmodulin 2 elicited cytoprotective signaling in endothelium.

If parmodulin 2 mediates its antithrombotic effect via stimulation of a cytoprotective pathway, then we would expect parmodulin-exposed endothelium to demonstrate antithrombotic properties beyond inhibition of thrombin generation. Exposure of endothelium to inflammatory mediators can stimulate recruitment of platelets from flowing blood (37). To determine whether parmodulin 2 affected platelet recruitment in a flow model under physiological shear rates, we evaluated the effect of parmodulin 2 in bioengineered microvessels. These vessels are constructed by collagen-coating 2-cm-long channels (400 μm width × 100 μm height) within a polydimethylsiloxane microfluidic chip and subsequently seeding the four walls of the chamber with endothelial cells (38, 39). Once the endothelium is grown to confluence, whole blood is perfused through the channels at 750 s^{-1}. Under the untreated conditions, platelets did not adhere to the endothelial surface (Fig. 1 *F* and *G*). If endothelial cells were first exposed to TNF-α before exposure to whole blood, however, then platelets accumulated on the endothelium (38). Exposure of endothelium to parmodulin 2 alone for 4 h had no effect on platelet accumulation on the endothelium (Fig. 1 *F* and *G*). In contrast, if the endothelium was first exposed to parmodulin 2, washed, and subsequently incubated with TNF-α, TNF-α–induced platelet accumulation was inhibited (Fig. 1 *F* and *G* and Movies S1–S4). Collectively, these data indicate that parmodulin exposure impairs the thrombotic response of endothelium to inflammatory stimuli without affecting blood coagulation. Given the ability of parmodulin 2 to inhibit both thrombin generation and platelet recruitment, the requirement for prolonged parmodulin 2 exposure to achieve antithrombotic activity, and the lack of anticoagulant activity, we evaluated the possibility that parmodulins stimulate cytoprotective signaling in endothelium.

Parmodulins Are Cytoprotective in Endothelial Cells. To determine whether parmodulins stimulated cytoprotective signaling in endothelium, we tested their effect on endothelial apoptosis. We also evaluated parmodulin 1 (9-methylene-4-alkyl-2,3,4,9-tetrahydro-1H-cyclopenta(b)quinolone; JF081204) (27) to determine whether cytoprotection was a class effect of parmodulins. Parmodulins inhibited apoptosis induced not only by thrombin but also by other agonists that act independently of PAR1, including TNF-α and staurosporine (Fig. 2 *A* and *B*). Incubation of HUVECs with parmodulin 1 or parmodulin 2 provided protection from apoptosis induced by exposure to TNF-α, thrombin, or staurosporine to an extent similar to that provided by APC (Fig. 2*B*). The ability of parmodulins to block TNF-α–induced apoptosis was also tested in a caspase-based assay of apoptosis, which confirmed the observation that parmodulins are cytoprotective (Fig. 2*C*).

The ability of parmodulins to inhibit apoptosis induced by TNF-α or staurosporine as well as by thrombin could result from off-target effects of the compounds. Alternatively, this cytoprotective effect could result from an APC-like activity at PAR1. To distinguish between these two possibilities, we inhibited PAR1 expression using siRNA directed at *F2R*. Knockdown of *F2R* (qRT-PCR: 99.35 ± 0.12%, $n = 3$; immunoblot analysis, Fig. S3) abrogated the ability of parmodulin 1, parmodulin 2, and APC to protect endothelial cells from TNF-α–induced apoptosis (Fig. 2*D*), confirming that parmodulin 1 and parmodulin 2 acted through PAR1 to prevent apoptosis in response to proinflammatory stimuli. The time course of parmodulin-mediated cytoprotection was also consistent with an APC-like effect, with protection of HUVECs from apoptosis requiring preincubation with parmodulins for >2 h (Fig. 2*E*).

Cytoprotective Signaling Elicited by Parmodulins. Previous studies have shown that PAR1 activation by APC involves its binding to the endothelial protein C receptor (EPCR) and changes in lipid rafts (40–42). Thus, it was unexpected that a small molecule could elicit cytoprotective signaling through PAR1 in endothelium. To determine how parmodulin 2 activated endothelial-cell cytoprotective responses, we evaluated proximal signal transduction induced by parmodulin 2. Cleavage of PAR1 by APC stimulates Akt phosphorylation at serine 473 in endothelial cells (18). Exposure of endothelium to parmodulin 2 resulted in Akt-S473 phosphorylation without significantly affecting total Akt levels (Fig. 3 *A* and *B* and Fig. S4 *A* and *B*). Evaluation of the subcellular localization of phospho-Akt in endothelial cells exposed to parmodulin 2 showed that, while Akt in untreated cells was distributed in the nucleus and throughout the cytoplasm, phospho-Akt observed following parmodulin 2 exposure localized to perinuclear and plasma membranes (Fig. 3*A*). There was a distinct absence of phospho-Akt from the nucleus of endothelial cells exposed to parmodulin 2. Induction of Akt phosphorylation was relatively rapid, occurring within 30 min of exposure (Fig. S4*C*). Since Akt is phosphorylated downstream of PI3K, we determined whether the PI3K inhibitors wortmannin and LY294002 blocked parmodulin-2–induced Akt phosphorylation. Both antagonists potently inhibited Akt phosphorylation following parmodulin 2 exposure (Fig. 3*B* and Fig. S5). PI3K phosphorylation stimulated by parmodulin 2 was visualized using an antiphospho-PI3K antibody that detects phosphorylation at residue Y607 on the p85 subunit of PI3K (43), confirming that parmodulin 2 signals through PI3K (Fig. 3*C*). The demonstration that parmodulins stimulate cytoprotective signaling via a PI3K/Akt-mediated pathway raises the question of whether this pathway also accounts for the antithrombotic activity of parmodulin 2 on endothelial cells. To evaluate this possibility, we incubated endothelial cells with parmodulin 2 in the presence of wortmannin. Wortmannin did not interfere with the factor Xa assay. However, it did inhibit the protective effect of parmodulin 2, reversing the ability of parmodulin 2 to block TNF-α–induced factor Xa activation (Fig. S7).

Parmodulins act at the cytoplasmic face of PAR1. Their biased antagonist activity relies on their ability to affect some downstream G-protein–coupled signaling pathways (e.g., Gαq), but not others (e.g., $G\alpha_{13}$) (29). The effect of either APC or parmodulin 2 exposure on Gβγ-mediated signaling has not previously been evaluated. However, Gβγ can stimulate PI3K (44–46)

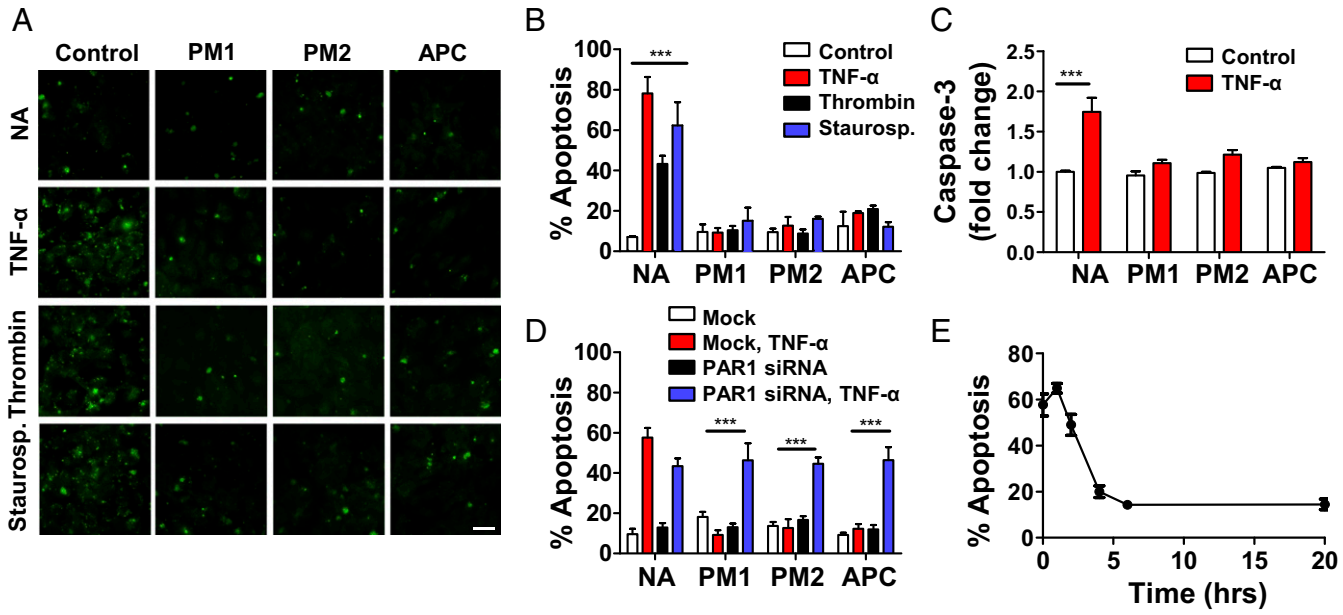

Fig. 2. A biased PAR1 agonist is cytoprotective in endothelial cells. (*A* and *B*) HUVECs were exposed to vehicle, PM1 (10 μM), PM2 (3 μM), or APC (10 μg/mL) for 4 h before exposure to buffer alone (NA), TNF-α (10 ng/mL), thrombin (1 U/mL), or staurosporine (10 μM) for an additional 4 h. Samples were evaluated for apoptosis by YO-PRO-1 staining (green) using fluorescence microscopy. (*A*) Representative images of YO-PRO-1 staining. (Scale bar: 25 μm.) (*B*) Quantification of the percentage of apoptotic cells. Data represent mean ± SEM (n = 4–5). Two-way ANOVA with Bonferroni's multiple comparison tests was used to compare groups. ***$P < 0.001$. (*C*) HUVECs were exposed to vehicle, PM1 (10 μM), PM2 (10 μM), or APC (5 μg/mL) for 4 h before exposure to buffer alone (NA) or TNF-α (50 ng/mL). Samples were evaluated for apoptosis using an antibody that detects cleaved caspase-3 as described in *Materials and Methods*. Fold change in relative fluorescence unit is depicted versus control-treated cells. Data represent the mean ± SEM (n = 6). Two-way ANOVA with Bonferroni posttests was used to compare groups. ***$P < 0.001$. (*D*) HUVECs were transfected with *F2R*-targeted siRNA (black, blue) or mock-transfected (white, red). Following confirmation of knockdown, samples were exposed to vehicle (NA), PM1 (10 μM), PM2 (3 μM), or APC (10 μg/mL) for 4 h before exposure to buffer or TNF-α (10 ng/mL) for an additional 4 h. Percentage of apoptotic cells was determined by fluorescence microscopy. Data represent the mean ± SEM (n = 4–5). Two-way ANOVA with Bonferroni posttests was used to compare groups. ***$P < 0.001$. (*E*) Time course of parmodulin-2–mediated protection from staurosporine-induced apoptosis. HUVECs were preincubated with PM2 (3 μM) for various times followed by exposure to staurosporine (10 μM) for an additional 4 h. The percentage of apoptotic cells was determined by fluorescence microscopy. Data represent the mean ± SEM (n = 6–7).

and parmodulin-2–activated Akt phosphorylation is mediated by PI3K (Fig. 3*B*). We therefore evaluated the possibility that parmodulin 2 stimulates PI3K via Gβγ. Gallein (M119) was used in these assays to inhibit Gβγ (47). Exposure to gallein blocked Akt phosphorylation stimulated by either parmodulin 2 or APC in endothelial cells (Fig. 3*D*). Incubation with gallein also inhibited parmodulin-2–mediated activation of PI3K (Fig. 3 *C* and *E* and Fig. S6*A*). In contrast, gallein failed to block angiopoietin-1–induced activation of PI3K, demonstrating that gallein was not directly inhibiting PI3K activation (Fig. S6 *B* and *C*). Involvement of Gβγ was not specific to parmodulin 2, as APC showed similar sensitivity to gallein (Fig. 3 *C*–*E*). Taken together, these studies indicate that binding of parmodulins to the cytosolic surface of PAR1 elicits dissociation or modulation of the Gβγ subunit of PAR1, which stimulates PI3K activation with phosphorylation of Akt in perinuclear and plasma membranes (Fig. 3*F*).

Effects of Parmodulins on Gene Transcription. Although signaling induced by parmodulins occurs within minutes following exposure, endothelial-cell cytoprotection is not achieved until hours after exposure to either parmodulins (Figs. 1 *D* and *E* and 2*D*) or APC (20, 36). One of the seminal observations supporting the premise that the protective effect of APC is mediated through its role in endothelial function was that APC modifies endothelial-cell gene transcription (14, 20). APC induces the up-regulation of cytoprotective genes and blocks the up-regulation of genes induced by inflammatory cytokines such as TNF-α (20, 36). To evaluate the effect of parmodulins on endothelial gene expression, transcript profiling of >30,000 genes was performed in HUVECs exposed to vehicle alone, parmodulin 2, TNF-α, or parmodulin 2 followed by TNF-α. TNF-α elicited the up-regulation of 748 genes. Parmodulin 2 inhibited up-regulation of 107 of these genes by ≥1.5-fold (Fig. 4*A*). qRT-PCR confirmed that parmodulin 2 inhibited toll-like receptor 2 (TLR2; Fig. 4*B*) and matrix metalloproteinase 10 (MMP10; Fig. 4*C*) expression.

Since TNF-α mediates inflammatory signaling through activation of NF-κB, we determined the effect of parmodulin 2 on TNF-α–induced NF-κB transcription activation. Parmodulin 2 blocked TNF-α–induced expression of a GFP reporter construct under the control of a NF-κB–sensitive promoter, indicating that it acts in part by inhibiting signaling to NF-κB (Fig. 4*D*). Parmodulin 1, parmodulin 2, and APC showed similar inhibition of TNF-α–induced NF-κB transcription activation (Fig. 4*D*).

Parmodulin 2 Stimulates Up-Regulation of Stanniocalcin-1. Transcript profiling also identified a smaller subset of transcripts that were up-regulated upon exposure to parmodulin 2 alone (Fig. 4*A*). Among this subset, *STC1*, which encodes for stanniocalcin-1, was of special interest since it had previously been shown to mediate cytoprotection in endothelial cells (48, 49). Real-time PCR confirmed that parmodulin 2 induced up-regulation of *STC1* at 4 h (Fig. 5*A*). Evaluation of protein expression demonstrated increased synthesis of stanniocalcin-1 by both immunoblot analysis (Fig. 5*B*) and immunofluorescence (Fig. 5*C* and Fig. S8 *A* and *B*). To test the premise that parmodulin 2 stimulated stanniocalcin-1 expression downstream of the Gβγ/PI3K/Akt pathway, we evaluated the effect of inhibitors of this pathway on parmodulin-2–induced expression of stanniocalcin-1. Preincubation of endothelial cells with gallein to block Gβγ, wortmannin to inhibit PI3K, or GSK69063 to block Akt interfered with parmodulin-2–mediated

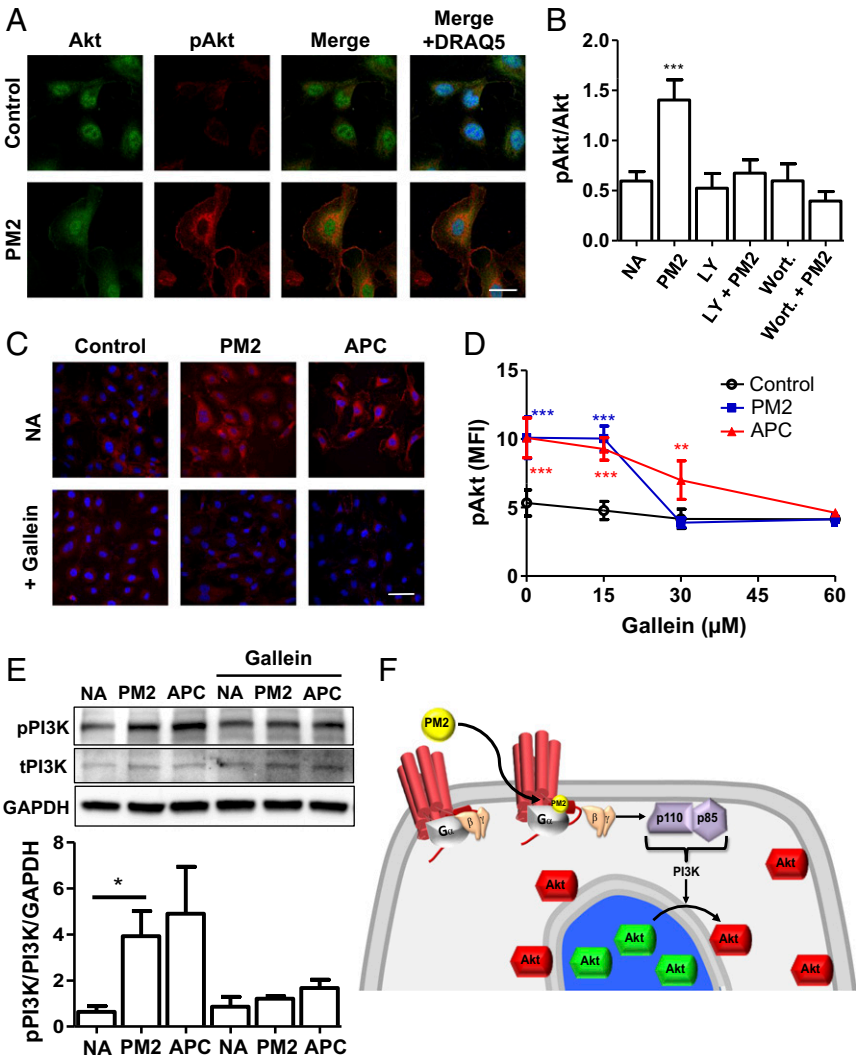

Fig. 3. Parmodulins stimulate an APC-like signaling pathway. (*A*) HUVECs were exposed to either vehicle or 3 μM PM2 and stained using an anti-Akt antibody (green), a phospho-Akt antibody (red), and DRAQ5 (blue) to visualize nuclei. Samples were then evaluated using three-color confocal immunofluorescence microscopy. (Scale bar: 25 μm.) (*B*) HUVECs were incubated with vehicle (NA), 0.1 μM wortmannin (Wort), or 50 μM LY294002 (LY) and subsequently exposed to either vehicle or PM2 as indicated. Samples were analyzed for phospho-Akt using confocal immunofluorescence microscopy, and staining intensity was quantified using Image J. Data represent mean ± SEM ($n = 5$). One-way ANOVA with Bonferroni posttest was used to compare groups. ***$P < 0.001$. (*C–E*) HUVECs were incubated in the presence or absence of gallein for 30 min. Samples were subsequently exposed to control, PM2, or APC for 4 h. (*C*) Cells were stained using a phospho-PI3K antibody and evaluated using confocal immunofluorescence microscopy. (Scale bar: 50 μm.) (*D*) Quantification of the inhibition by gallein of Akt phosphorylation induced using either PM2 (blue) or APC (red) compared with control (black). Data represent mean fluorescent intensities ± SEM ($n = 3$). One-way ANOVA with Bonferroni posttests was used to compare PM2- and APC-treated groups to control. **$P < 0.01$; ***$P < 0.001$. (*E*) Immunoblot analysis demonstrating the inhibition of PM2- and APC-induced PI3K phosphorylation by gallein (60 μM). Data represent mean ± SEM ($n = 4$). One-way ANOVA with Bonferroni posttests was used to compare groups to NA: *$P < 0.05$. (*F*) Model illustrating the proposed role of Gβγ in PM2 signaling. PM2 associates with the cytoplasmic face of PAR1 displacing Gβγ and enabling it to activate PI3K. PI3K then phosphorylates Akt that is localized to perinuclear and plasma membranes.

up-regulation of stanniocalcin-1 (Fig. 5 *C* and *D*). These data indicate that parmodulin 2 up-regulation of stanniocalcin-1 is downstream of the PI3K/Akt pathway.

The induction of stanniocalcin-1 expression by parmodulin 2 raised the question of whether stanniocalcin-1 functions in parmodulin-2–mediated cytoprotection. To evaluate this question, stanniocalcin-1 expression was reduced using siRNA directed at *STC1*. Knockdown of *STC1* (qRT-PCR: 79.47 ± 4.30%, $n = 3$; and immunoblot analysis, Fig. S8*C*) blocked the protective effect of parmodulin 1, parmodulin 2, and APC on TNF-α–induced apoptosis (Fig. 5*E*). These studies indicate that both parmodulins and APC achieve cytoprotection, at least in part, through the activity of stanniocalcin-1. To determine whether parmodulin 2 causes up-regulation of stanniocalcin-1 in vivo, we analyzed the effect of parmodulin 2 infusion into mice on endothelial stanniocalcin-1. Analysis of stanniocalcin-1 staining of aortic slices confirmed that parmodulin 2 infusion results in up-regulation of endothelial stanniocalcin-1 in mice (Fig. 5 *F* and *G*). These results confirm that parmodulin 2 reaches its cellular target (i.e., endothelial PAR1) when infused into mice and that parmodulin 2 causes up-regulation of stanniocalcin-1 in vivo.

Parmodulin 2 Protects Against Thromboinflammatory Injury in Vivo. Thrombosis and inflammation are two closely linked host defense systems that share common cellular and molecular effectors. PAR1 is an important receptor in the endothelial response to thromboinflammatory signals. To determine whether cytoprotection by parmodulins is observed in live animals, we evaluated

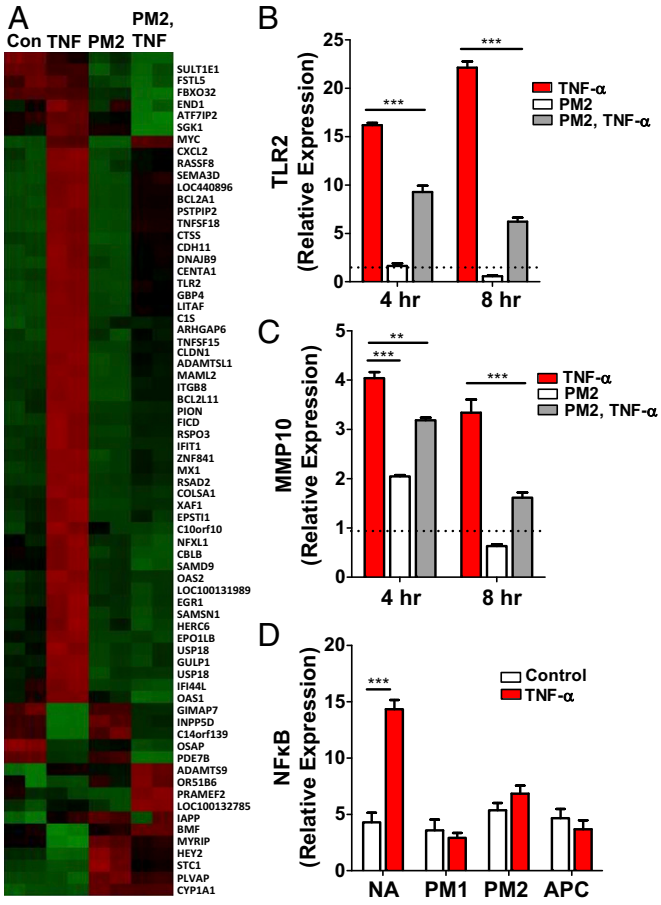

Fig. 4. Gene expression profiling of endothelial cells following exposure to parmodulin 2. (*A*) Transcript profiling of HUVECs was performed using GeneChip Human Gene 1.0 ST Affymetrix chip following incubation of endothelium with vehicle alone (NA), 10 ng/mL TNF-α (TNF), 3 μM PM2 (PM2), or PM2 followed by TNF-α (PM2, TNF). (*B* and *C*) HUVECs were exposed to vehicle (red) or PM2 (white, gray) for 4 h before exposure to buffer (white) or TNF-α (red, gray) for an additional 4 h. Samples were subsequently evaluated for either (*B*) TLR2 mRNA or (*C*) MMP10 mRNA using qRT-PCR. Dashed line represents the value of samples exposed to vehicle alone. Data represent fold difference of triplicate samples (mean ± SEM) compared with the control (NA) at 4 h. (*D*) Transcriptional activation downstream from NF-κB was detected using a GFP-based reporter system. HUVECs were exposed to vehicle (NA), 10 μM PM1, 3 μM PM2, or 5 μg/mL APC for 4 h before exposure to TNF-α for an additional 4 h. NF-κB expression was analyzed using immunofluorescence microscopy. Data represent mean ± SEM (n = 4–5). (*B–D*) Two-way ANOVA with Bonferroni's multiple comparison tests was used. $^{**}P < 0.01$; $^{***}P < 0.001$.

the effect of parmodulin 2 on endothelial-cell responses to thromboinflammatory stimuli. Parmodulin 2 was infused into mice before LPS exposure, and soluble E-selectin and von Willebrand factor (VWF) levels were monitored. Quantification of soluble E-selectin showed that parmodulin 2 protected against LPS-induced E-selectin release from endothelium (Fig. 6*A*). Pretreatment with parmodulin 2 also blocked LPS-induced increases in VWF release (Fig. 6*B*). Infusion of APC has been shown to reduce leukocyte adhesion and rolling in animal models of vascular inflammation (50, 51). We next evaluated whether parmodulin 2 affected leukocyte rolling in surgery-inflamed cremaster venules. Infusion of 10 mg/kg parmodulin 2 reduced rolling flux on surgery-inflamed venules by 59% compared with infusion of vehicle (Fig. 6*C*).

Thrombotic responses to injury are exaggerated in the setting of inflammation, providing a means to evaluate the effect of cytoprotective agents on thromboinflammatory response. To test the effect of parmodulin 2 in ameliorating thromboinflammatory responses, we monitored platelet accumulation and fibrin formation in response to laser injury in the setting of LPS exposure. Both platelet accumulation and fibrin formation following laser-induced injury of cremaster arterioles were substantially enhanced in the setting of LPS exposure compared with vehicle alone (Fig. 7 and Fig. S9 *A* and *B*). Infusion of parmodulin markedly impaired platelet accumulation at sites of vascular injury and also reduced fibrin formation (Fig. 7 *A–C*). Furthermore, in the setting of LPS exposure, infusion of parmodulin 2 reduced platelet accumulation to levels observed in vehicle control (Fig. 7*B* and Fig. S9*A*) and also significantly reduced fibrin formation in this setting (Fig. 7*C* and Fig. S9*B*). In contrast, parmodulin 2 failed to inhibit thrombin-induced aggregation of mouse platelets even at low concentrations of thrombin (Fig. S9 *C–E*). These results indicate an antithrombotic effect of parmodulin 2 at the level of the endothelium and are consistent with the studies (Fig. 1) evaluating platelet accumulation and thrombin generation in vitro.

Discussion

Parmodulins are a class of small molecules that stimulate PAR1-mediated cytoprotection and represent a fundamentally different approach to pharmacological modulation of PAR1. By acting at the cytosolic face of PAR1, these compounds have antagonist properties achieving relatively rapid (<30 m) inhibition of signaling mediated through Gαq, but not $G\alpha_{13}$, and agonist properties stimulating Gβγ to elicit cytoprotective signaling. This mechanism differs from that of orthosteric antagonists, such as vorapaxar, which associate tightly with the substrate binding site and block all downstream signaling including cytoprotective signaling (7, 52). Although parmodulins stimulate cytoprotective signaling, they are also unlike APC, since they have no anticoagulant effect on factor V or VIII. In this regard, they are more similar to APCs engineered with mutations that impair cleavage of factor V or VIII (23, 53–56). The most clinically advanced of these is 3K3A-APC, which has little anticoagulant activity and enhanced cytoprotective activity (57, 58). It has proved to be very effective in several animal models and is currently in human trials for treatment of stroke (59). Parmodulins differ from APC and its anticoagulant-deficient mutants, however, in that they do not interact with other APC-binding partners such as EPCR (14), ApoER2 (60), or PAR3 (61). Parmodulins also differ in that they do not pose even a theoretical risk of antibody formation to endogenous APC. The ability of parmodulins to block Gαq-mediated signaling in platelets and endothelium further distinguishes these compounds from APC and its anticoagulant-deficient mutants. Thus, parmodulins are unique as molecular probes to interrogate PAR1-mediated cytoprotective signaling and as leads for therapeutics targeting the PAR1 cytoprotective pathway.

While proximal activation mechanisms of APC and parmodulins differ significantly, parmodulins appear to have co-opted downstream signal transduction mechanisms similar to those used in the PAR1-dependent cytoprotective pathway activated by APC. Binding of APC to EPCR (14) orients APC on the endothelial surface (40, 41, 62) such that APC can cleave the PAR1 N terminus primarily at the nonconical Arg-46 site (18). Binding of APC to EPCR also promotes recruitment of G-protein–coupled receptor kinase 5, which phosphorylates the cytoplasmic tail of PAR1 following APC-mediated cleavage (40, 41, 62, 63). Parmodulins bypass the requirements for EPCR association and cleavage of the PAR1 extracellular domain by associating directly with the cytoplasmic face of PAR1 (29). We show that inhibition of Gβγ function by gallein (47) blocks parmodulin-mediated phosphorylation of Akt and PI3K (Fig. 3 *C–E*). The fact that gallein inhibits PI3K phosphorylation induced by parmodulin, but not that induced by angiopoietin-1, indicates that it is acting at Gβγ and not nonspecifically or at PI3K (Fig. S6 *B* and *C*). A potential mechanism for parmodulin activation of cytoprotective signaling is that association of parmodulin with the cytoplasmic

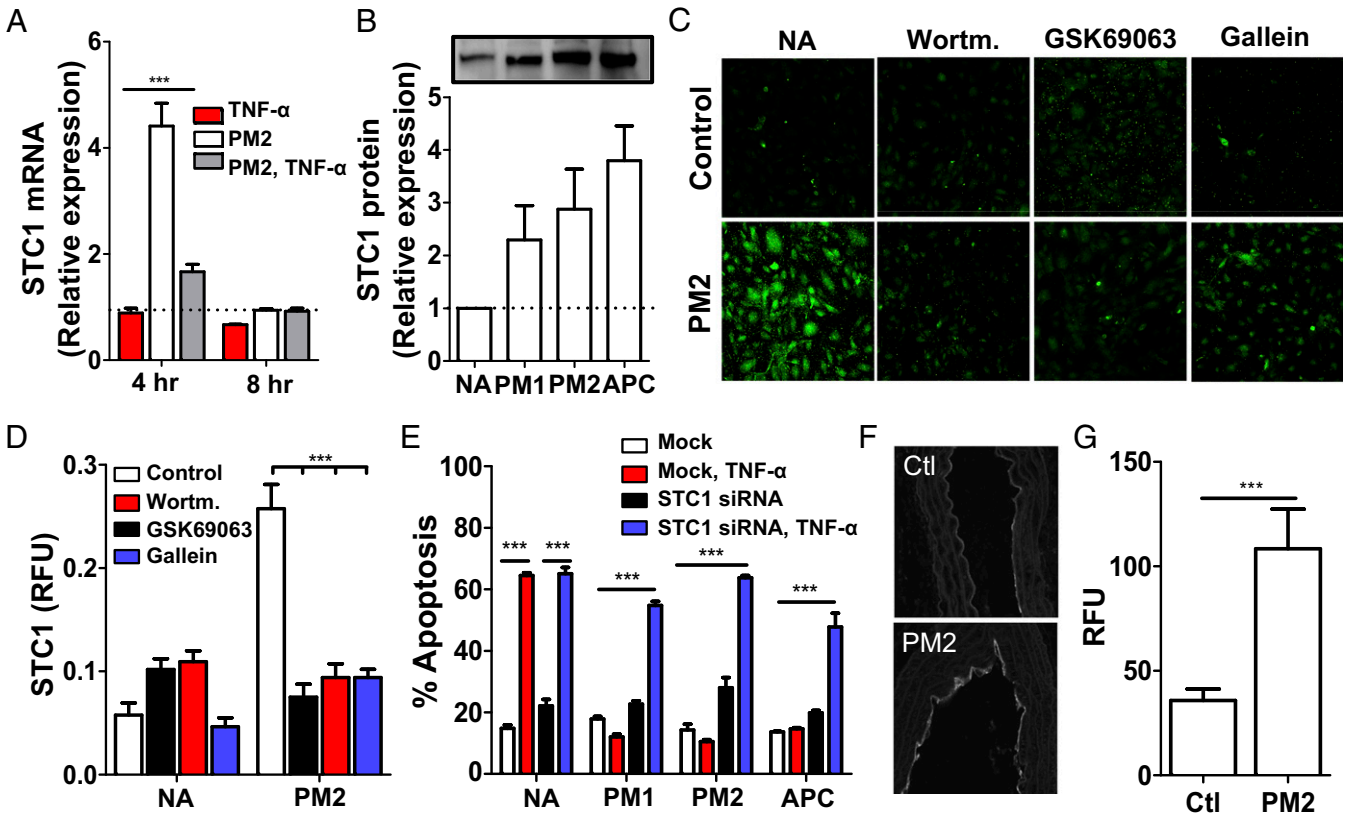

Fig. 5. Stanniocalcin-1 is up-regulated by parmodulin exposure and is essential for cytoprotection. (*A*) HUVECs were exposed to vehicle or 3 μM PM2 for 4 h before exposure to buffer or 10 ng/mL TNF-α. Subsequently, samples were evaluated for *STC1* mRNA expression using qRT-PCR. Dashed line represents value of samples exposed to vehicle alone. Data represent fold difference of triplicate samples (mean ± SEM) compared with the no addition control. Two-way ANOVA with Bonferroni's multiple comparison tests was used. ***$P < 0.001$. (*B*) Quantification of immunoblot analysis for stanniocalcin-1 (STC1) protein. Data represent fold difference (mean ± SEM) compared with no addition (NA) control at 4 h ($n = 4$). *Inset* shows a representative immunoblot of HUVEC lysates following exposure to vehicle, PM1, PM2, or APC. (*C* and *D*) HUVECs were preincubated with wortmannin (Wortm.; 0.1 μM), Akt inhibitor GSK69063 (0.2 μM), or gallein (60 μM) for 30 min before incubation with vehicle or PM2 (10 μM) in the absence or presence of inhibitors for an additional 4 h. Following incubation, HUVECs were stained with anti-STC1 antibody (green) and DAPI (blue) and evaluated by immunofluorescence microscopy. (*C*) Representative images. (Magnification: 60×.) (*D*) Quantification of STC1 expression as calculated by the ratio of relative fluorescence units (RFUs) versus number of cells. Data represent mean ± SEM ($n = 6$). Two-way ANOVA with Bonferroni's multiple comparison tests was used. ***$P < 0.001$. (*E*) HUVECs were transfected with siRNA targeted at *STC1* (black, blue) or mock-transfected (white, red). Following knockdown, samples were exposed to vehicle, PM1, PM2, or APC for 4 h before exposure to buffer (white, black) or 10 ng/mL TNF-α (red, blue) for an additional 4 h. The percentage of apoptotic cells was determined using fluorescence microscopy. Data indicate the mean ± SEM ($n = 4$–5). Two-way ANOVA with Bonferroni posttests was used. ***$P < 0.001$. (*F*) Representative image of confocal immunofluorescence microscopy of aorta from mice infused with vehicle (Control, or Ctl) or 10 mg/kg PM2 and stained using anti-STC1 antibody. (Magnification: 5×.) (*G*) Immunofluorescence quantitation of STC1 staining in aortas of mice infused with vehicle ($n = 181$ fields) or 10 mg/kg parmodulin 2 ($n = 222$ fields). Unpaired *t* test was used to compare PM2 to control (Ctl). ***$P < 0.001$.

face of PAR1 either displaces or modifies G-protein association in a manner that activates Gβγ function (Fig. 3*F*). Activation of Gβγ is known to stimulate PI3K signaling (44–46). We also show that APC requires activation of Gβγ (Fig. 3). The consequences of these activities in endothelium are stimulation of PI3K/Akt-mediated cytoprotective signaling. Previous studies have demonstrated a role for β-arrestin in APC-mediated cytoprotective signaling (10, 62). Future studies will evaluate the relative roles of β-arrestin and Gβγ in proximal signaling mechanisms elicited by APC and parmodulins.

Although APC and parmodulins interact with PAR1 via entirely distinct mechanisms, the cytoprotective program induced by parmodulins and APC has important similarities. Both APC and parmodulins elicit cytoprotection through changes in gene expression. These changes include inhibition of NF-κB–mediated transcriptional activation (Fig. 4), as has been observed for APC (14, 20). In addition, parmodulin-mediated up-regulation of specific genes was also observed. Among these genes was *STC1*. Previous transcriptional profile studies suggested that *STC1* is up-regulated following exposure of endothelium to APC (36). We show that stanniocalcin-1 protein is up-regulated in endothelium following exposure to either APC or parmodulins and that up-regulation of stanniocalin-1 is dependent on PI3K/Akt signaling (Fig. 5), as has been shown in mesenchymal stem cells and breast cancer cells (64, 65). Moreover, the protective effect of APC and parmodulins is dependent on stanniocalcin-1. Stanniocalcin-1 is known to be antiinflammatory in several cell types including endothelial cells (48, 49). Our studies demonstrate its importance in PAR1-mediated cytoprotection.

Beyond uncovering previously unrecognized aspects of PAR1 protective signaling, studies using parmodulins show that PAR1-mediated cytoprotection is antithrombotic at the level of endothelium, in addition to being antiapoptotic, barrier protective, and antiinflammatory. Parmodulins inhibit factor Xa and thrombin generation resulting from activation of endothelium by LPS or TNF-α (Fig. 1 *A* and *E*), presumably by interfering with up-regulation of tissue factor (33, 34). The inhibitory activity of parmodulins was not mediated by inhibition of Gαq, which is rapid, but rather by the stimulation of cytoprotection, which depends on transcriptional regulation and requires prolonged incubation with

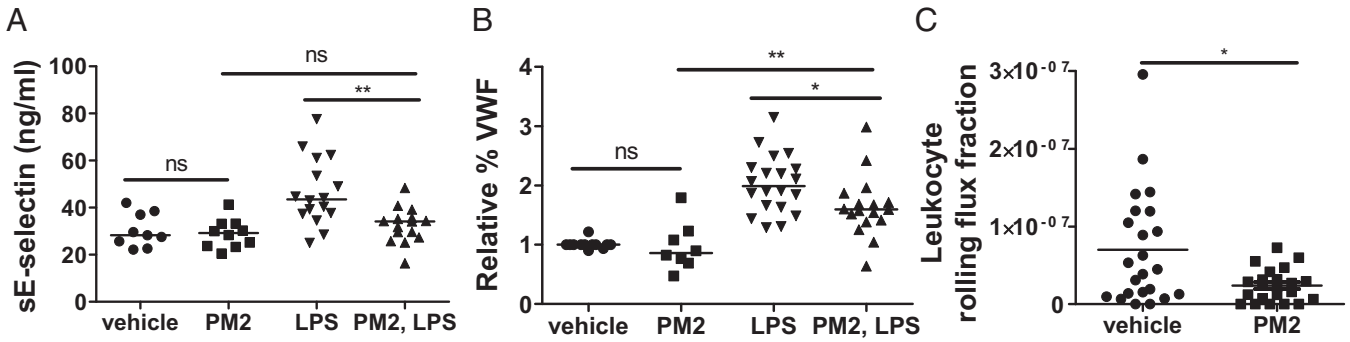

Fig. 6. Parmodulins interfere with activation of endothelium in vivo. Mice were infused with either vehicle or PM2 (10 mg/kg) 3 h before LPS exposure and an additional bolus injection of vehicle or PM2 just before saline or 10 mg/kg LPS injection. After a 3-h incubation period, plasma was obtained from mice and evaluated for either (*A*) soluble E-selectin (sE-selectin) or (*B*) VWF using ELISA. Data represent mean ± SEM of number of mice treated with vehicle ($n = 9$), PM2 ($n = 9$), LPS ($n = 15$), and PM2, LPS ($n = 16$). Statistical significance was determined using a Mann–Whitney test with a Hochberg's step-up method. $^*P < 0.05$; $^{**}P < 0.01$. (*C*) Mice were infused with either vehicle or 10 mg/kg PM2, and surgery-induced leukocyte rolling was monitored by intravital microscopy. Rolling flux was calculated as described in *Materials and Methods*. Data represent mean ± SEM of 22 (vehicle) and 23 (PM2) measurements. Mann–Whitney test was used to determine significance. $^*P < 0.05$. ns, nonsignificant.

parmodulins to achieve inhibition (Fig. S2 *G* and *H*). Endothelium incubated with parmodulins before exposure to TNF-α also shows substantially less recruitment of platelets from flowing blood (Fig. 1 *F* and *G*). In the latter studies, parmodulins were washed away before exposure of endothelium to whole blood, mitigating any direct effects of parmodulins on platelets. These results prove that isolated stimulation of cytoprotective signaling through PAR1 is able to mediate thromboprotection in endothelium, independent of direct anticoagulant or antiplatelet effects.

Evaluation of parmodulin effects on thrombus formation in vivo also demonstrates significant antithrombotic activity at the level of the endothelium. Parmodulin 2 does not block thrombin-induced

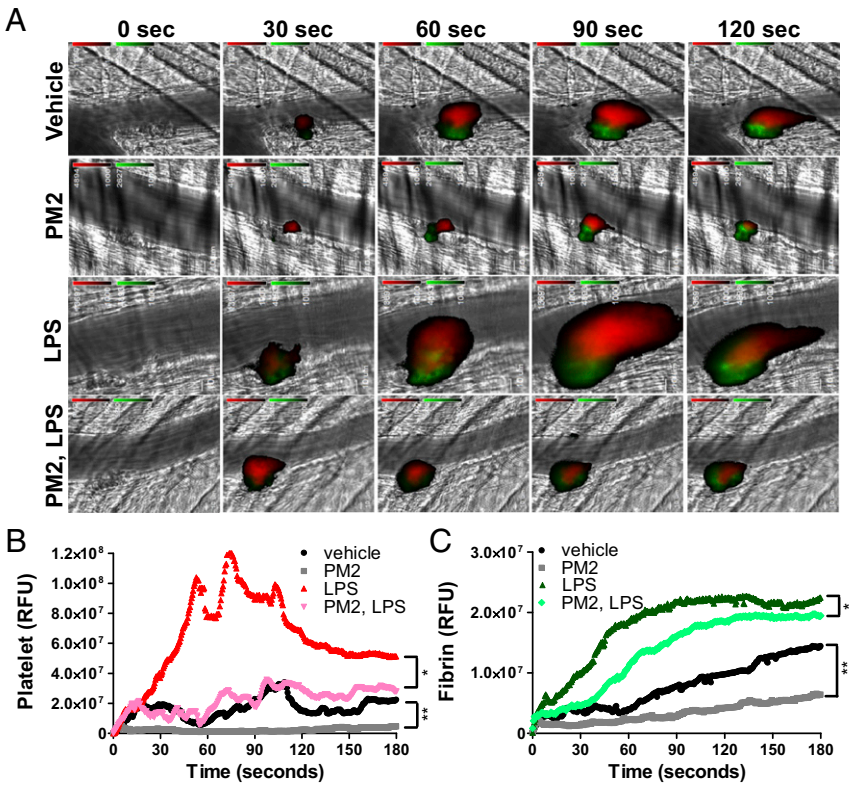

Fig. 7. Parmodulins are protective in the setting of thromboinflammation. (*A*) Mice were injected i.v. with vehicle or PM2 (5–10 mg/kg) 2.5 h before 10 mg/kg LPS administration i.p. and with an additional bolus 0.5 h after LPS exposure. Thrombus formation was induced by endothelial laser injury in cremaster arterioles 1–3 h following LPS injection. Platelet (red) and fibrin (green) accumulation were monitored for 180 s using Dylight 647-labeled antiplatelet antibody (CD42b) and Dylight 488-labeled antifibrin antibody (59D8). Representative binarized images from a single thrombus are shown for vehicle, PM2, and LPS and PM2 followed by LPS. (*B* and *C*) Median integrated platelet and fibrin fluorescent intensities following laser injury were calculated for all thrombi in vehicle ($n = 37$), PM2 ($n = 37$), LPS ($n = 30$), and PM2 followed by LPS ($n = 38$) experiments. (Magnification: 60×.) (*B*) Median integrated platelet fluorescent intensities are indicated for vehicle (black), PM2 (gray), LPS alone (red), PM2 followed by LPS (pink). (*C*) Median integrated platelet fluorescent intensities are indicated for vehicle (black), PM2 (gray), LPS alone (dark green), and PM2 followed by LPS (light green). A Kruskal–Wallis test with multiple comparisons was used. $^*P < 0.05$. $^{**}P < 0.01$.

activation of mouse platelets (Fig. S9), which relies on PAR4 stimulation. In contrast, parmodulins demonstrate protective effects on endothelium in vitro and inhibit inflammation-induced release of von Willebrand factor and E-selectin in vivo, confirming that parmodulins engage endothelial PAR1 in mice. In the setting of laser injury, parmodulins inhibit fibrin generation as well as platelet accumulation in the presence or absence of LPS exposure (Fig. 7). In contrast, platelet inhibitors such as eptifibatide inhibit platelet accumulation with relatively little effect on fibrin generation in our laser-induced thrombus formation model (66, 67). This observation indicates an antithrombotic effect of parmodulins at the level of the endothelium. Our results underscore the potential of targeting the PAR1 cytoprotective pathway in thromboinflammatory disorders.

A limitation of our in vivo studies is that we cannot assess the bleeding risk of parmodulins in humans. Parmodulin 2 did not prolong bleeding following tail snip in mice (29). However, the human and murine PAR systems differ in platelets: mice have a PAR4 dominant system (with PAR3 acting as a coreceptor), while PAR signaling in human platelets depends on PAR1 and PAR4. Thus, we cannot extrapolate from murine studies and cannot assess the bleeding risk that parmodulins pose in humans. PAR1 inhibition by orthosteric inhibitors such as vorapaxar is associated with bleeding (68–70). However, while vorapaxar is a much more potent antagonist that shows essentially irreversible inhibition, parmodulin-mediated inhibition of platelet function is readily reversible (29). Clinical trials using parmodulins will be required to evaluate their potential bleeding risk. A second limitation of these studies is that, while they provide for proof-of-concept for the use of parmodulins in thromboinflammatory disease, they do not provide guidance with regard to specific indications or the timing of parmodulin use. Parmodulins have a slow onset of action and may be better suited for primary or secondary prevention than for acute treatment of thromboinflammatory disorders.

These studies provide proof-of-principle for targeting the cytoplasmic domains of a GPCR to selectively stimulate downstream signaling. GPCRs remain the most commonly targeted receptor class for marketed therapeutics. Nearly all GPCR-targeted pharmaceuticals act at the extracellular face of the receptor. Parmodulins achieve selective modulation of G-protein signaling by targeting the cytosolic face of PAR1. Endothelial PAR1 is a particularly good target for such a strategy because of the wide range of its signaling repertoire; it couples to several downstream G proteins and can stimulate either inflammatory or antiinflammatory signaling. However, many GPCRs stimulate both beneficial and deleterious signaling, depending on the ligand and context of stimulation. The ability to selectively control signaling pathways at the level of G-protein–coupled signaling could represent a significant advance in controlling these highly abundant and frequently targeted receptors.

Materials and Methods

Thrombin and FXa Generation Assays. HUVECs were grown in Corning CellBIND 96-well plates (VWR) until confluent. Cells were treated for 3 h with a mixture containing LPS (100 ng/mL), LPS-binding protein (LBP) (10 ng/mL), and sCD14 (100 ng/mL) or 4 h with TNF (10 ng/mL). In indicated experiments, cells were pretreated with vehicle or parmodulin 2 (3 μM) for 4 h before exposure to LPS or TNF in the absence or presence of wortmannin (100 nM). For experiments with APC, cells were preincubated with APC (10 nM) for 4 h before LPS or TNF stimulation (factor Xa) or incubated with LPS or TNF in the absence or presence of APC (thrombin). For thrombin generation, medium was removed, and 80 μL of plasma with 5 mM glycine–proline–arginine–proline peptide (ThermoFisher Scientific) and 20 μL of Hepes-buffered saline was added. Calcium (3 mM) was added to initiate thrombin generation. Following a 20-min incubation period, thrombin generation was measured in plasma using a fluorogenic thrombin substrate (SN-20, Haematologic Technologies) diluted in PBS with 5 mM EDTA. Fluorescence was measured every minute for a total of 20 min. For factor Xa assays, HUVECs were washed three times with prewarmed (37 °C) Hepes buffered saline (HBS) containing 1% BSA and 5 mM calcium (HBS-BSA). Factor Xa generation was measured by adding purified factor X (100 nM) and factor VIIa (0.67 nM) to the cells in HBS-BSA buffer in the presence of a chromogenic factor Xa substrate [200 μM; CS-11(22); Biophen]. Absorbance at 405 nm was measured every minute for 2 h using the SPECTRAmax 340 PC plate reader (Molecular Devices). The rate of thrombin substrate and factor Xa substrate cleavage was converted to units/mL.

Bioengineered Microvessel Thrombosis Assay. A customized microfluidic device was made using photolithography with polydimethylsiloxane (PDMS) molding and used as described (38, 39). Briefly, each PDMS microfluidic chip consisting of six microvessels was pretreated with 100 μg/mL rat-tail collagen type I (Corning) diluted in PBS. After overnight incubation, channels were washed with medium and HUVECs were seeded (8–10 × 10^5 cells/mL). The devices containing the HUVEC suspension were held upside down and incubated for 20 min, and then the device was returned to its original orientation and a new HUVEC suspension was introduced into the device and incubated for 8 h to obtain a confluent monolayer on all four walls of the microchannel. HUVECs were treated with parmodulin 2 (30 μM) for 4 h followed by treatment with TNF-α (recombinant from *Escherichia coli*, Sigma; 50 ng/mL) for 4 h. Citrated whole blood supplemented with 100 mM calcium and 75 mM magnesium (1:10 ratio) was perfused through the engineered microvessels at 750 s^{-1} using a pump. Platelets were labeled with 10 μg/mL human CD41-PE antibody (ThermoFisher Scientific) and visualized using Zeiss Axio Observer (LD Plan Neufluar 10×, N.A. 0.4 objective) with a Hamamatsu ORCA C11440 CMOS digital camera.

Informed Consent and Institutional Review Board Approval. Blood drawing and preparation of human platelets was performed according to a protocol approved by the institutional review board of Beth Israel Deaconess Medical Center. All participants gave written informed consent. C57BL/6J mice (male; 8–12 wk) were obtained from The Jackson Laboratory. Animal care and experimental procedures were performed in accordance with and under the approval of the Beth Israel Deaconess Medical Center Institutional Animal Care and Use Committee.

Statistics. GraphPad prism 7 was used for statistical data analysis. The following tests were used were applicable: two-tailed unpaired *t* tests, one-way and two-way ANOVAs with Bonferroni posttests, and the Kruskal–Wallis test. A Hochberg step-up method was used for analyzing data of in vivo mouse experiments. Sample sizes and statistical tests are indicated in the figure legends.

For additional materials and methods, see *SI Materials and Methods*.

ACKNOWLEDGMENTS. This work was funded by the National Heart, Lung, and Blood Institute (Grants HL125275, HL112809, HL135775, T32 HL007917, and T32 HL116324-02) and by the Wyss Institute for Biologically Inspired Engineering at Harvard University.

1. Vu TK, Hung DT, Wheaton VI, Coughlin SR (1991) Molecular cloning of a functional thrombin receptor reveals a novel proteolytic mechanism of receptor activation. *Cell* 64:1057–1068.
2. Griffin CT, Srinivasan Y, Zheng YW, Huang W, Coughlin SR (2001) A role for thrombin receptor signaling in endothelial cells during embryonic development. *Science* 293: 1666–1670.
3. Trivedi V, et al. (2009) Platelet matrix metalloprotease-1 mediates thrombogenesis by activating PAR1 at a cryptic ligand site. *Cell* 137:332–343.
4. Sen P, et al. (2013) Factor VIIa bound to endothelial cell protein C receptor activates protease activated receptor-1 and mediates cell signaling and barrier protection. *Blood* 117:3199–3208.
5. Tressel SL, et al. (2011) A matrix metalloprotease-PAR1 system regulates vascular integrity, systemic inflammation and death in sepsis. *EMBO Mol Med* 3:370–384.
6. Kahn ML, et al. (1998) A dual thrombin receptor system for platelet activation. *Nature* 394:690–694.
7. Zhang C, et al. (2012) High-resolution crystal structure of human protease-activated receptor 1. *Nature* 492:387–392.
8. Ayoub MA, et al. (2007) Real-time analysis of agonist-induced activation of protease-activated receptor 1/Galphai1 protein complex measured by bioluminescence resonance energy transfer in living cells. *Mol Pharmacol* 71:1329–1340.
9. Ayoub MA, Trinquet E, Pfleger KD, Pin JP (2010) Differential association modes of the thrombin receptor PAR1 with Galphai1, Galpha12, and beta-arrestin 1. *FASEB J* 24: 3522–3535.
10. Soh UJ, Trejo J (2011) Activated protein C promotes protease-activated receptor-1 cytoprotective signaling through β-arrestin and dishevelled-2 scaffolds. *Proc Natl Acad Sci USA* 108:E1372–E1380.

11. Dowal L, Flaumenhaft R (2010) Targeting platelet G-protein coupled receptors (GPCRs): Looking beyond conventional GPCR antagonism. *Curr Vasc Pharmacol* 8: 140–154.
12. Canto I, Soh UJK, Trejo J (2012) Allosteric modulation of protease-activated receptor signaling. *Mini Rev Med Chem* 12:804–811.
13. van der Poll T, Levi M (2012) Crosstalk between inflammation and coagulation: The lessons of sepsis. *Curr Vasc Pharmacol* 10:632–638.
14. Riewald M, Petrovan RJ, Donner A, Mueller BM, Ruf W (2002) Activation of endothelial cell protease activated receptor 1 by the protein C pathway. *Science* 296: 1880–1882.
15. Riewald M, et al. (2001) Gene induction by coagulation factor Xa is mediated by activation of protease-activated receptor 1. *Blood* 97:3109–3116.
16. Camerer E, Kataoka H, Kahn M, Lease K, Coughlin SR (2002) Genetic evidence that protease-activated receptors mediate factor Xa signaling in endothelial cells. *J Biol Chem* 277:16081–16087.
17. Sen P, et al. (2011) Factor VIIa bound to endothelial cell protein C receptor activates protease activated receptor-1 and mediates cell signaling and barrier protection. *Blood* 117:3199–3208.
18. Mosnier LO, Sinha RK, Burnier L, Bouwens EA, Griffin JH (2012) Biased agonism of protease-activated receptor 1 by activated protein C caused by noncanonical cleavage at Arg46. *Blood* 120:5237–5246.
19. Franscini N, et al. (2004) Gene expression profiling of inflamed human endothelial cells and influence of activated protein C. *Circulation* 110:2903–2909.
20. Joyce DE, Gelbert L, Ciaccia A, DeHoff B, Grinnell BW (2001) Gene expression profile of antithrombotic protein C defines new mechanisms modulating inflammation and apoptosis. *J Biol Chem* 276:11199–11203.
21. Griffin JH, Zlokovic BV, Mosnier LO (2015) Activated protein C: Biased for translation. *Blood* 125:2898–2907.
22. Mosnier LO, et al. (2009) Hyperantithrombotic, noncytoprotective Glu149Ala-activated protein C mutant. *Blood* 113:5970–5978.
23. Kerschen EJ, et al. (2007) Endotoxemia and sepsis mortality reduction by non-anticoagulant activated protein C. *J Exp Med* 204:2439–2448.
24. Schuepbach RA, Velez K, Riewald M, Dc W (2012) Activated protein C up-regulates procoagulant tissue factor activity on endothelial cells by shedding the TFPI Kunitz 1 domain. *Blood* 117:6338–6346.
25. Solymoss S, Tucker MM, Tracy PB (1988) Kinetics of inactivation of membrane-bound factor Va by activated protein C. Protein S modulates factor Xa protection. *J Biol Chem* 263:14884–14890.
26. Vehar GA, Davie EW (1980) Preparation and properties of bovine factor VIII (antihemophilic factor). *Biochemistry* 19:401–410.
27. Dowal L, et al. (2011) Identification of an antithrombotic allosteric modulator that acts through helix 8 of PAR1. *Proc Natl Acad Sci USA* 108:2951–2956.
28. Dockendorff C, et al. (2012) Discovery of 1,3-diaminobenzenes as selective inhibitors of platelet activation at the PAR1 receptor. *ACS Med Chem Lett* 3:232–237.
29. Aisiku O, et al. (2015) Parmodulins inhibit thrombus formation without inducing endothelial injury caused by vorapaxar. *Blood* 125:1976–1985.
30. Guessous F, et al. (2005) Shiga toxin 2 and lipopolysaccharide induce human microvascular endothelial cells to release chemokines and factors that stimulate platelet function. *Infect Immun* 73:8306–8316.
31. Ghanekar A, et al. (2004) Endothelial induction of fgl2 contributes to thrombosis during acute vascular xenograft rejection. *J Immunol* 172:5693–5701.
32. Clauss M, et al. (1990) Vascular permeability factor: A tumor-derived polypeptide that induces endothelial cell and monocyte procoagulant activity, and promotes monocyte migration. *J Exp Med* 172:1535–1545.
33. Herbert JM, Savi P, Laplace MC, Lale A (1992) IL-4 inhibits LPS-, IL-1 beta- and TNF alpha-induced expression of tissue factor in endothelial cells and monocytes. *FEBS Lett* 310:31–33.
34. Bevilacqua MP, et al. (1986) Recombinant tumor necrosis factor induces procoagulant activity in cultured human vascular endothelium: Characterization and comparison with the actions of interleukin 1. *Proc Natl Acad Sci USA* 83:4533–4537.
35. Bannerman DD, Goldblum SE (2003) Mechanisms of bacterial lipopolysaccharide-induced endothelial apoptosis. *Am J Physiol Lung Cell Mol Physiol* 284:L899–L914.
36. Riewald M, Ruf W (2005) Protease-activated receptor-1 signaling by activated protein C in cytokine-perturbed endothelial cells is distinct from thrombin signaling. *J Biol Chem* 280:19808–19814.
37. Babinska A, et al. (2002) F11-receptor (F11R/JAM) mediates platelet adhesion to endothelial cells: Role in inflammatory thrombosis. *Thromb Haemost* 88:843–850.
38. Jain A, et al. (2016) Assessment of whole blood thrombosis in a microfluidic device lined by fixed human endothelium. *Biomed Microdevices* 18:73.
39. Jain A, et al. (2017) Primary human lung alveolus-on-a-chip model of intravascular thrombosis for assessment of therapeutics. *Clin Pharmacol Ther*, 10.1002/cpt.742.
40. Russo A, Soh UJ, Paing MM, Arora P, Trejo J (2009) Caveolae are required for protease-selective signaling by protease-activated receptor-1. *Proc Natl Acad Sci USA* 106:6393–6397.
41. Bae JS, Yang L, Manithody C, Rezaie AR (2007) The ligand occupancy of endothelial protein C receptor switches the protease-activated receptor 1-dependent signaling specificity of thrombin from a permeability-enhancing to a barrier-protective response in endothelial cells. *Blood* 110:3909–3916.
42. Bae JS, Yang L, Rezaie AR (2008) Lipid raft localization regulates the cleavage specificity of protease activated receptor 1 in endothelial cells. *J Thromb Haemost* 6: 954–961.
43. Hou X, et al. (2014) Advanced glycation endproducts trigger autophagy in cadiomyocyte via RAGE/PI3K/AKT/mTOR pathway. *Cardiovasc Diabetol* 13:78.
44. Metjian A, Roll RL, Ma AD, Abrams CS (1999) Agonists cause nuclear translocation of phosphatidylinositol 3-kinase gamma. A Gbetagamma-dependent pathway that requires the p110gamma amino terminus. *J Biol Chem* 274:27943–27947.
45. Brock C, et al. (2003) Roles of G beta gamma in membrane recruitment and activation of p110 gamma/p101 phosphoinositide 3-kinase gamma. *J Cell Biol* 160:89–99.
46. Maier U, et al. (2000) Gbeta 5gamma 2 is a highly selective activator of phospholipid-dependent enzymes. *J Biol Chem* 275:13746–13754.
47. Bonacci TM, et al. (2006) Differential targeting of Gbetagamma-subunit signaling with small molecules. *Science* 312:443–446.
48. Chen C, Jamaluddin MS, Yan S, Sheikh-Hamad D, Yao Q (2008) Human stanniocalcin-1 blocks TNF-alpha-induced monolayer permeability in human coronary artery endothelial cells. *Arterioscler Thromb Vasc Biol* 28:906–912.
49. Chakraborty A, et al. (2007) Stanniocalcin-1 regulates endothelial gene expression and modulates transendothelial migration of leukocytes. *Am J Physiol Renal Physiol* 292:F895–F904.
50. Gupta A, et al. (2007) Activated protein C ameliorates LPS-induced acute kidney injury and downregulates renal INOS and angiotensin 2. *Am J Physiol Renal Physiol* 293: F245–F254.
51. Hoffmann JN, et al. (2004) Microhemodynamic and cellular mechanisms of activated protein C action during endotoxemia. *Crit Care Med* 32:1011–1017.
52. Olivier C, Diehl P, Bode C, Moser M (2013) Thrombin receptor antagonism in antiplatelet therapy. *Cardiol Ther* 2:57–68.
53. Mosnier LO, Yang XV, Griffin JH (2007) Activated protein C mutant with minimal anticoagulant activity, normal cytoprotective activity, and preservation of thrombin activable fibrinolysis inhibitor-dependent cytoprotective functions. *J Biol Chem* 282: 33022–33033.
54. Mosnier LO, Gale AJ, Yegneswaran S, Griffin JH (2004) Activated protein C variants with normal cytoprotective but reduced anticoagulant activity. *Blood* 104:1740–1744.
55. Harmon S, et al. (2008) Dissociation of activated protein C functions by elimination of protein S cofactor enhancement. *J Biol Chem* 283:30531–30539.
56. Andreou AP, et al. (2015) Protective effects of non-anticoagulant activated protein C variant (D36A/L38D/A39V) in a murine model of ischaemic stroke. *PLoS One* 10: e0122410.
57. Gale AJ, Tsavaler A, Griffin JH (2002) Molecular characterization of an extended binding site for coagulation factor Va in the positive exosite of activated protein C. *J Biol Chem* 277:28836–28840.
58. Guo H, et al. (2009) Species-dependent neuroprotection by activated protein C mutants with reduced anticoagulant activity. *J Neurochem* 109:116–124.
59. Griffin JH, Mosnier LO, Fernández JA, Zlokovic BV (2016) 2016 Scientific Sessions Sol Sherry Distinguished Lecturer in Thrombosis: Thrombotic stroke: Neuroprotective therapy by recombinant-activated protein C. *Arterioscler Thromb Vasc Biol* 36: 2143–2151.
60. Yang XV, et al. (2009) Activated protein C ligation of ApoER2 (LRP8) causes Dab1-dependent signaling in U937 cells. *Proc Natl Acad Sci USA* 106:274–279.
61. Guo H, et al. (2004) Activated protein C prevents neuronal apoptosis via protease activated receptors 1 and 3. *Neuron* 41:563–572.
62. Roy RV, Ardeshirylajimi A, Dinarvand P, Yang L, Rezaie AR (2016) Occupancy of human EPCR by protein C induces β-arrestin-2 biased PAR1 signaling by both APC and thrombin. *Blood* 128:1884–1893.
63. Tiruppathi C, et al. (2000) G protein-coupled receptor kinase-5 regulates thrombin-activated signaling in endothelial cells. *Proc Natl Acad Sci USA* 97:7440–7445.
64. Ono M, et al. (2015) Mesenchymal stem cells correct inappropriate epithelial-mesenchyme relation in pulmonary fibrosis using stanniocalcin-1. *Mol Ther* 23: 549–560.
65. Jeon M, Han J, Nam SJ, Lee JE, Kim S (2016) STC-1 expression is upregulated through an Akt/NF-κB-dependent pathway in triple-negative breast cancer cells. *Oncol Rep* 36: 1717–1722.
66. Vandendries ER, Hamilton JR, Coughlin SR, Furie B, Furie BC (2007) Par4 is required for platelet thrombus propagation but not fibrin generation in a mouse model of thrombosis. *Proc Natl Acad Sci USA* 104:288–292.
67. Jasuja R, Furie B, Furie BC (2010) Endothelium-derived but not platelet-derived protein disulfide isomerase is required for thrombus formation in vivo. *Blood* 116: 4665–4674.
68. Tricoci P, et al.; TRACER Investigators (2012) Thrombin-receptor antagonist vorapaxar in acute coronary syndromes. *N Engl J Med* 366:20–33.
69. Morrow DA, et al.; TRA 2P–TIMI 50 Steering Committee and Investigators (2012) Vorapaxar in the secondary prevention of atherothrombotic events. *N Engl J Med* 366:1404–1413.
70. Capodanno D, et al. (2012) Safety and efficacy of protease-activated receptor-1 antagonists in patients with coronary artery disease: A meta-analysis of randomized clinical trials. *J Thromb Haemost* 10:2006–2015.